Raman-scattering study of $CuGeO_3$ in the spin-Peierls phase

Haruhiko Kuroe and Tomoyuki Sekine
Department of Physics, Sophia University, 7-1 Kioi-cho, Chiyoda-ku, Tokyo 102, Japan

Masashi Hase, Yoshitaka Sasago, and Kunimitsu Uchinokura
Department of Applied Physics, The University of Tokyo, 7-3-1 Hongo, Bunkyo-ku, Tokyo 113, Japan

Hironao Kojima, Isao Tanaka, and Yuki Shibuya
Institute of Inorganic Synthesis, Yamanashi University, Kofu-shi, Yamanashi 400, Japan
(Received 7 July 1994)

Phonons and magnetic excitations were studied as a function of temperature in the spin-Peierls phase of an inorganic material $CuGeO_3$ by Raman scattering. All of the phonon Raman peaks observed at room temperature can be assigned on condition that the crystal symmetry is D_{2h}^5 (*Pbmm*). Five peaks intrinsic to the spin-Peierls state were observed at 30, 105, 228, 370, and 818 cm^{-1} in the spin-Peierls phase. The temperature dependence of the frequency of the 30-cm^{-1} peak agrees approximately with $2\Delta(T)$, where $\Delta(T)$ is the spin-Peierls gap. The Raman spectrum between 0 and 300 cm^{-1} was compared with the density of states of the magnetic excitons. The 105- and 228-cm^{-1} peaks were assigned to two-magnetic-exciton Raman scattering. The peaks at 370 and 818 cm^{-1} were assigned to one-phonon Raman scattering of the folded A_g modes, which occurs due to the formation of a dimerization in the spin-Peierls phase.

I. INTRODUCTION

Recently, Hase, Terasaki, and Uchinokura[1] reported that the magnetic susceptibilities of $CuGeO_3$ in all directions drop to small values exponentially below T_{SP} =14 K, and they assigned this phenomenon to a spin-Peierls phase transition. An anomalous specific heat was observed near T_{SP},[2] and it has been thermodynamically confirmed that the phase transition occurs around this temperature. The decrease of the critical temperature T_{SP} is proportional to H^2 when the magnetic field H is applied.[1] These results have been observed in the spin-Peierls system of organic materials. In addition, it was also reported that the magnetic phase diagram of $CuGeO_3$ agrees with the experimental results of typical organic spin-Peierls materials and theoretical calculation.[3] Although the measured susceptibility above 14 K shows characteristics of a one-dimensional (1D) antiferromagnetic spin system,[1] the susceptibility does not agree quantitatively with the theoretical one of a 1D antiferromagnet calculated by Bonner and Fisher.[4]

In the spin excitations (magnetic excitons) of the spin-Peierls phase, a gap opens between the spin-singlet and excited states, accompanied by a periodic lattice dimerization along the magnetic chain. Nishi, Fujita, and Akimitsu[5] observed the energy gap in the magnetic-exciton spectrum by means of an inelastic-neutron-scattering experiment below 14 K. The gap reached a value of 2.1 meV (24.4 K) at 0 K, which is consistent with the result of a magnetic susceptibility measurement (24 K).[1]

Very recently, Kamimura *et al.*[6] observed superlattice reflections due to lattice dimerization by means of electron diffraction. Moreover, the satellite reflections were observed by means of neutron diffraction by Hirota *et al.*[7] and Pouget *et al.*[8] and by means of x-ray diffraction.[8] A precise neutron-diffraction measurement of Hirota *et al.*[7] confirmed the static displacement of Cu and O in the chain in the $2a \times b \times 2c$ superlattice.

The crystal structure of $CuGeO_3$ at room temperature was studied by Völlenkle, Wittmann, and Howotny[9] by means of x-ray diffraction before the discovery of the spin-Peierls transition, and determined the space group D_{2h}^5 (*Pbmm*, which is equivalent to *Pmma* in the standard orientation). $CuGeO_3$ possesses an orthorhombic unit cell with the lattice constants of 4.81, 8.47, and 2.941 Å along the a, b, and c axes, respectively,[9] which contains two edge-sharing CuO_6 octahedra with two Cu-O bonds of 2.766 Å and four of 1.942 Å. A 1D antiferromagnetic chain consists of two O^{2-} ions and a Cu^{2+} ion with a spin $S = 1/2$ in a primitive cell of the chain. These spins interact antiferromagnetically with each other. $CuGeO_3$ also contains a vertex-sharing GeO_3 tetrahedral chain aligned along the c axis.

Adams and Fletcher[10] observed twelve Raman-active modes and eleven IR-active modes in $CuGeO_3$ powder, and stated that the symmetry of the lattice is D_{2h}^5. We reported a preliminary result of Raman scattering in single-crystal $CuGeO_3$ and stated that our result supports the crystal symmetry of D_{2h}^5 reported by Völlenkle, Wittmann, and Howotny[9] from the polarization characteristics.[11]

Sugai[12] measured the Raman spectra in the spin-

Peierls phase and observed five new Raman peaks at 30, 105, 228, 370, and 819 cm^{-1}. He claimed that a soft-phonon mode which appeared at 34 cm^{-1} at room temperature was frozen at T_{SP}, and its frequency increased again with decreasing temperature below T_{SP} and reached 30 cm^{-1} at 5 K.

Recently Udagawa *et al.*[13] observed five Raman peaks at 27, 107, 230, 370, and 820 cm^{-1} which appeared in the spin-Peierls phase of $CuGeO_3$. They suggested that the three low-frequency peaks are due to magnetic excitations. This assignment was based only on the fact that the energies of these peaks were near twice those of the magnetic excitations, but they measured the temperature dependence of neither the frequencies nor intensities of these peaks.

Although the spin-Peierls phase transition was established in $CuGeO_3$ by the observation of the lattice dimerization and the gap of magnetic excitons, it seems to us that the origin of the new Raman peaks in the spin-Peierls phase has not been firmly determined. The explanations about the new Raman peaks at low temperatures which were given by Sugai and Udagawa *et al.* contradicted each other. Detailed measurements of the intensities and the frequencies of these Raman peaks as a functions of temperature are, therefore, required to understand the nature of the Raman peaks intrinsic to the spin-Peierls phase.

In this paper, we present the temperature dependence of Raman spectra in $CuGeO_3$, in particular below T_{SP}, and clarify the origin of the Raman peaks in the spin-Peierls phase.

II. EXPERIMENTAL DETAILS

The sample was prepared by a floating-zone method. The single-crystal sample was transparent and blue in color, and was cleaved easily on layers in the *bc* plane. The dimension of the sample was $2 \times 5 \times 3\,mm^3$ parallel to the *a*, *b*, and *c* axes, respectively.

Raman-scattering experiments were carried out using 4880- and 5145-Å lines of an Ar^+ ion laser. In order to eliminate plasma lines and get a complete linear polarization, we made the laser light pass through two filters and a polarizer and then the laser light was incident on the sample in a cryostat. The scattered light was dispersed by a Jobin-Yvon U1000 double-grating monochromator and detected by a photon counting system. Whole system was controlled with a microcomputer.

To measure the Raman spectra around liquid-He temperature, we used a continuous-flow-type cryostat (Janis-Research SuperTran-VP). The temperature of the sample was controlled by two PID temperature controllers, one of which controls the temperature at the vaporizer and the other at the sample holder, independently. The temperature of the sample was equal to that of the sample holder within ± 0.1 K.

To reduce the intensity of Rayleigh scattering, Raman-scattering measurements were carried out in a right-angle scattering geometry. The *bc* plane of the sample was attached to the sample holder by diluted varnish, and the light was incident on the *ab* or *ac* plane. Since the sample was transparent and cooled directly by a cold He gas, the local temperature rise due to the incident light was negligible.

III. RESULTS AND DISCUSSION

First, we measured the polarized Raman spectra at room temperature. Twelve independent Raman peaks indicated by arrows were observed at 298 K, as shown in Fig. 1. Let us show that the crystal belongs to D_{2h}^5 symmetry at room temperature. We choose the crystal axes as the space-group notation *Pbmm* adopted by Völlenkle, Wittmann, and Howotny.[9] The crystal axes *a*, *b*, and *c* were already written according to this notation. At room temperature, the long-wavelength optical phonons of $CuGeO_3$ can be classified as

$$\underline{4A_g + 4B_{1g} + 3B_{2g} + B_{3g}} + 2A_u + 3B_{1u} + 5B_{2u} + 5B_{3u} .$$

Among them the underlined symmetric modes are Raman active and their Raman tensors are written as

$$A_g : \begin{pmatrix} a & & \\ & b & \\ & & c \end{pmatrix} , \quad B_{1g} : \begin{pmatrix} & d & \\ d & & \\ & & \end{pmatrix} ,$$

$$B_{2g} : \begin{pmatrix} & & e \\ & & \\ e & & \end{pmatrix} , \quad B_{3g} : \begin{pmatrix} & f & \\ f & & \\ & & \end{pmatrix} .$$

The number of the Raman peaks observed in the present experiment and the polarization characteristics indicate that the space group of $CuGeO_3$ at room temperature is D_{2h}^5. Four Raman peaks at 184, 339, 592, and 857 cm^{-1} are observed strongly in the $c(b,b)a$ geometry and are assigned to A_g modes. Four B_{1g} modes at 114, 221,

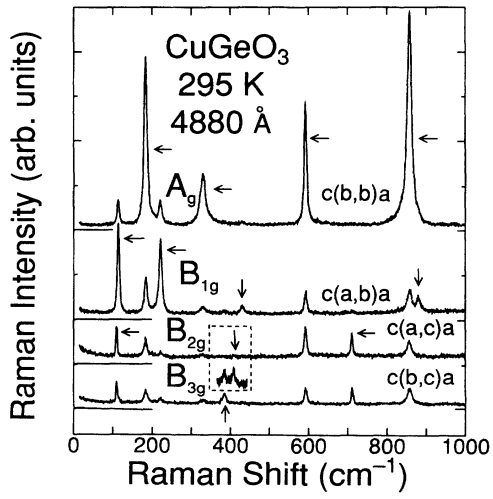

FIG. 1. Raman spectra of $CuGeO_3$ at room temperature. Peaks which are allowed in the polarization geometry are denoted by arrows.

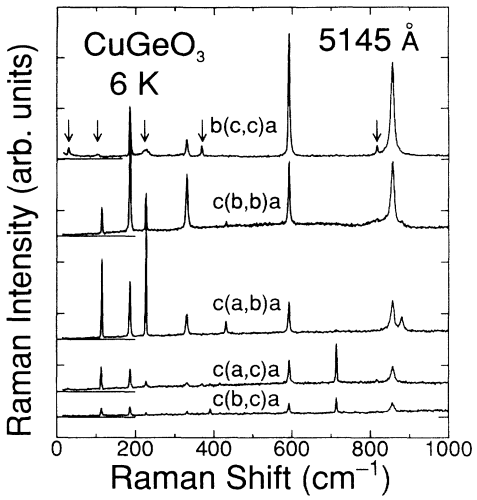

FIG. 2. Raman spectra of $CuGeO_3$ below T_{SP}. Five peaks observed only in the spin-Peierls phase appear in the $b(c,c)a$ geometry and are indicated by arrows. Unreproducible backgrounds were observed when the 4880-Å line was used as an incident light. Therefore the spectra were measured by using 5145-Å line. The origin of the backgrounds is thought to be photoluminescence due to impurities.

430, and 879 cm^{-1} appear mainly in the $c(a,b)a$ geometry, three B_{2g} modes at 110, 409, and 710 cm^{-1} in the $c(a,c)a$ geometry, and a B_{3g} mode at 385 cm^{-1} in the $c(b,c)a$ geometry. The breakdown of the polarization characteristics, however, was observed in several Raman modes. For example, the B_{1g} modes have considerably strong intensities in the $c(b,b)a$ geometry. Since we cut the sample along the ab and ac planes, perpendicular to the plane of cleavage, there might be strains in the sample. We consequently found all of the Raman-active modes at room temperature.

Next, we measured the polarized Raman spectra at 6 K to confirm that the crystal structure changes in the spin-Peierls phase. The experimental result using the 5145-Å line of Ar^+ ion laser is shown in Fig. 2. Although the main characteristic spectra are similar to those at room temperature, five peaks intrinsic to the spin-Peierls phase appear at 30, 105, 228, 370, and 818 cm^{-1} at 6 K. These peaks are observed strongly in the $b(c,c)a$ geometry.

Then we measured the temperature dependence of these new peaks, and the results are shown in Fig. 3. All of these peaks disappear around $T_{SP} = 14$ K with increasing temperature. The peak around 113 cm^{-1} in Fig. 3(b) comes from phonon Raman scattering, and it was observed also at room temperature.

One can see that three low-frequency peaks are not symmetric. The 105- and the 228-cm^{-1} peaks have a tail on the lower-energy side, and the 30-cm^{-1} peak has a tail on the higher-energy one. Since the asymmetry is small, the Raman peak was fitted by the following spectral function using the method of least squares:

$$I(\omega) = \frac{k^2\Gamma}{(\omega-\omega_0)^2+\Gamma^2}\left[n\left(\frac{\omega}{\alpha}\right)+1\right]^{\alpha} + \text{background}\,, \tag{1}$$

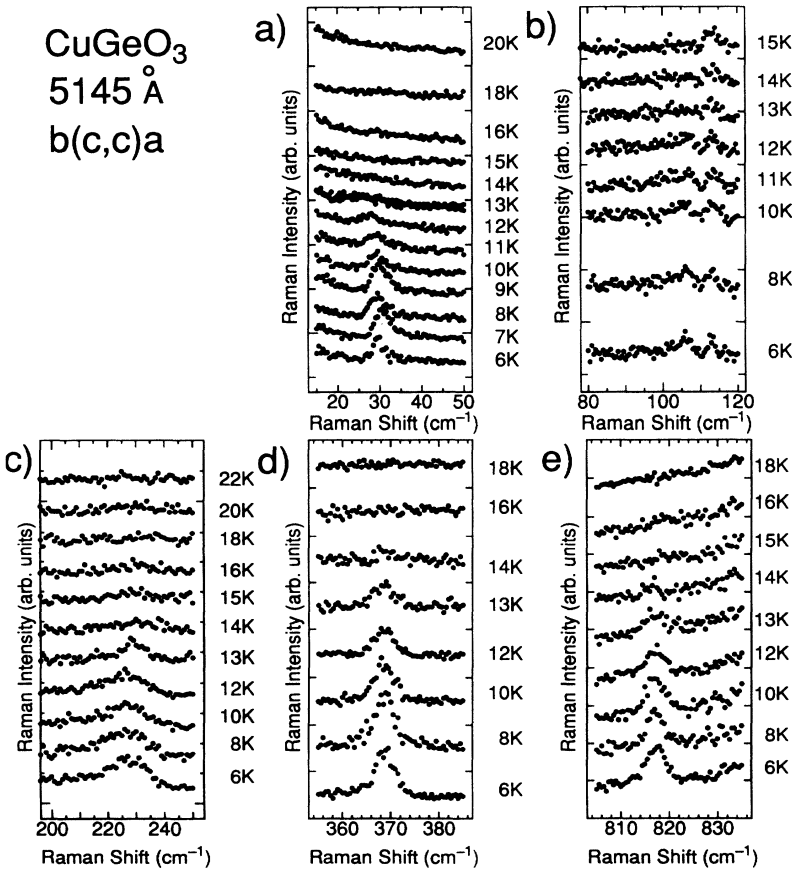

FIG. 3. Temperature dependence of Raman spectra of the new peaks at 30 (a), 105 (b), 228 (c), 370 (d), and 818 (e) cm^{-1}. A peak near 113 cm^{-1} in (b) is not intrinsic to the spin-Peierls phase.

where ω_0, Γ, and k are the frequency of the peak position, the damping constant, and the coupling coefficient, respectively, and $n(\omega)$ is the Bose factor. Here $\alpha = 1$ corresponds to the first-order Raman process, and $\alpha = 2$ to the second-order one. The integrated intensity is given as

$$\int_0^\infty (I(\omega) - \text{background})d\omega \approx \left[n\left(\frac{\omega_0}{\alpha}\right) + 1\right]^\alpha k^2\pi. \tag{2}$$

The temperature dependence of k^2 and ω_0 of the four peaks observed below T_{SP} is shown in Fig. 4. We assumed the first-order Raman process ($\alpha = 1$) in the cases of the 370- and 818-cm^{-1} peaks and the second-order one ($\alpha = 2$) in the cases of the 30- and 228-cm^{-1} peaks, and the reason of our assumptions will be discussed later. When the temperature increases, the k^2 of the peaks decrease, and become zero at T_{SP}. Since the 105-cm^{-1} peak is weak in intensity, and there is, moreover, a tail of the 113-cm^{-1} peak which is due to the one-phonon Raman process, we could not fit the observed 105-cm^{-1} peak by Eq. (1) precisely. But we can say that the peak position of the 105-cm^{-1} peak does not shift and its intensity decreases when the temperature approaches T_{SP}. The value of $\omega_0(T)$ of the 30-cm^{-1} peak shifts to lower energy when the temperature increased, while the others are nearly temperature independent.

Then we also plotted the temperature dependence of the peak energy $\omega_0(T)$ of the 30-cm^{-1} peak in Fig. 5 in units of meV to compare it with $\Delta(T)$ and $2\Delta(T)$, where $\Delta(T)$ is the spin-Peierls gap obtained by means of inelastic neutron scattering.[5] It was reported that the temperature dependence of the spin-Peierls gap cannot be described by BCS theory. The observed $\Delta(T)$ was fitted by the equation,

$$\Delta(T) = \Delta(0)\left(1 - \frac{T}{T_{SP}}\right)^\beta, \tag{3}$$

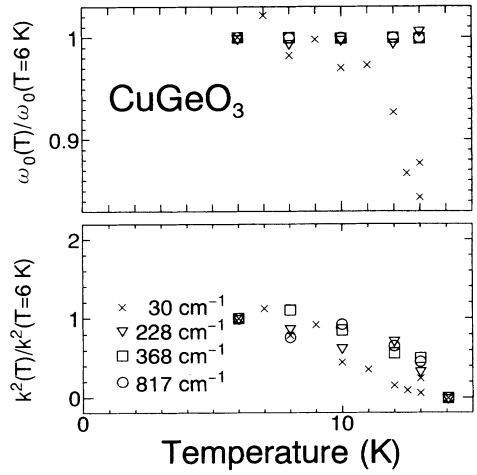

FIG. 4. Temperature dependence of $\omega_0(T)$ and $k^2(T)$ of the five new peaks. The first-order Raman process is assumed for the 370- and 818-cm^{-1} peaks, and the second-order Raman process is assumed for the 30- and 228-cm^{-1} peaks. All of them are normalized by the values at $T = 6$ K.

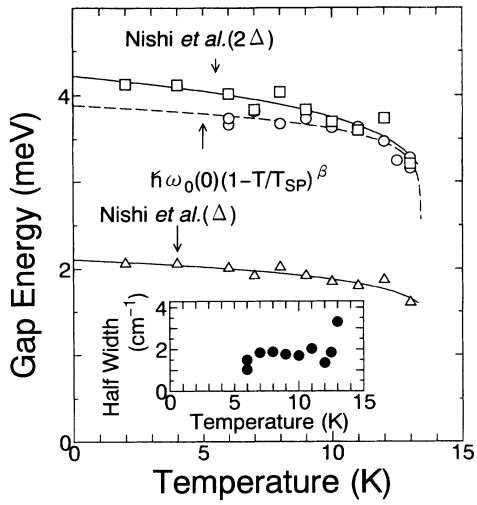

FIG. 5. Temperature dependence of $\omega_0(T)$ of the 30-cm^{-1} peak (circles). The spin-Peierls gaps $\Delta(T)$ and $2\Delta(T)$ obtained by the neutron-diffraction measurement are also plotted by triangles and squares, respectively, and the fitted solid curves were obtained by Nishi *et al.* (Ref. 5). A dashed curve denotes the fitted curve of our data. An inset shows the half width $2\Gamma(T)$.

where $\Delta(0) = 2.11$ meV, $T_{SP} = 14$ K, and $\beta = 0.093$.[5] One can see that $2\Delta(T)$ has almost the same temperature dependence as our result of $\omega_0(T)$ of the 30-cm^{-1} peak, although $\omega_0(T)$ is a little smaller than $2\Delta(T)$ at low temperatures. In antiferromagnets, the intensity of the two-magnon peak is generally larger than that of the one-magnon peak in the case of the Raman scattering,[14] and therefore we conclude tentatively that the 30-cm^{-1} peak corresponds to the 2Δ gap. The first-order Raman process of the magnetic exciton was not observed. If we fit our data to Eq. (3) [$2\Delta(0)$ is replaced by $\hbar\omega_0(0)$], we obtain the parameters $\hbar\omega_0(0) = 3.88$ meV, $T_{SP} = 13.3$ K, and $\beta = 0.051$. The result is shown by the dashed curve in Fig. 5. The half width $2\Gamma(T)$ of the peak in the inset of Fig. 5 increases—i.e., the peak becomes broad—when the temperature approaches T_{SP}.

We consider a two-magnetic-exciton process where a pair of magnetic excitons with momenta of $+\mathbf{q}$ and $-\mathbf{q}$ is created. Since the total momentum of this pair is 0, this two-magnetic-exciton process can be observed by Raman scattering. The Raman spectrum, therefore, reflects the density of states $D(\omega)$ of the magnetic exciton. Then we calculated the density of states from the following dispersion relation which was adopted by Nishi, Fujita, and Akimitsu:[5]

$$(\hbar\omega_{\mathbf{q}})^2 = \left\{\frac{\pi}{2}J_c + J_b + E_A - J_a(1 - \cos 2\pi h)\right\}^2 - \left(\frac{\pi}{2}J_c \cos 2\pi l + J_b \cos \pi k\right)^2, \tag{4}$$

where

$$\mathbf{q} = h\mathbf{a}^* + k\mathbf{b}^* + l\mathbf{c}^*. \tag{5}$$

Here J_a, J_b, and J_c are the exchange integrals along the a, b, and c axes, respectively, and $\mathbf{a}^*$, $\mathbf{b}^*$, and $\mathbf{c}^*$

are the reciprocal lattice vectors of the high-temperature phase. The uniaxial anisotropic magnetic energy E_A is used so as to fit the spin-Peierls energy gap. Nishi, Fujita, and Akimitsu obtained $J_c = 10.4$ meV, $J_b \approx 0.1J_c$, and $J_a \approx -0.01J_c$. Independently, we fitted their data again fixing J_c at 10.4 meV, and obtained that $J_a = -0.044$ meV, $J_b = 0.35$ meV, and $E_A = 0.13$ meV. We calculated $\hbar\omega_{\mathbf{q}}$ at about 150×10^6 points in reciprocal lattice space using the above-mentioned parameters. Since we consider the second-order Raman process, we plotted the calculated density of states $D(\omega/2)$ multiplied by $[n(\omega/2)+1]^2$ together with the observed Raman spectra at 6 K in Fig. 6.

Although the calculated curve (solid one) could represent the observed Raman spectrum qualitatively, in particular asymmetry of the peak, some problems remain in the quantitative agreement. First, the calculated curve does not show a peak, but the M_0-type singularity ($\propto \sqrt{\omega - 2\Delta}$) at $2\Delta \approx 30$ cm^{-1}. On the other hand, we observed a sharp peak with a small tail on the higher-energy side near 30 cm^{-1}. The formation of the peak near 2Δ can be explained in terms of the bound state of the two magnetic excitons because of the strong attractive interaction between two magnetic excitons with low excitation energy and the quasi-one-dimensionality of the spin system in $CuGeO_3$. In one-dimensional Heisenberg-XY spin systems, the spinless fermion representation of the Hamiltonian contains interaction terms between spinless fermions. Therefore the magnetic excitons are not independent excitations but they intrinsically interact with each other. We can easily show that the interaction between the two magnetic excitons (two spinless fermions and two spinless fermion holes) is attractive at least when the excitation energy is small ($\approx 2\Delta$). A bound state, split from the bottom of the continuous band, is formed. As is seen in Fig. 5, the frequency $\omega_0(T)$ of the 30-cm^{-1} peak is a little smaller than $2\Delta(T)$ obtained by inelastic neutron scattering at low temperatures. This fact is consistent with the bound-state model.

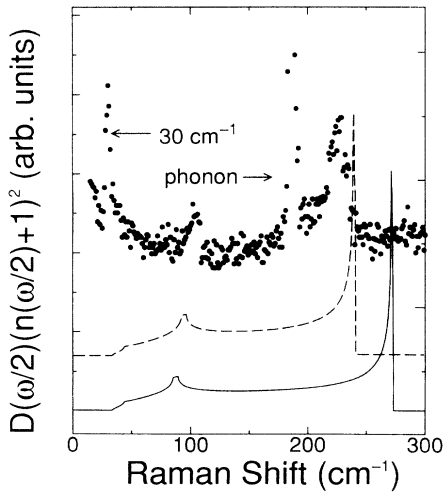

FIG. 6. Observed and calculated Raman spectra. Solid circles denote our data. A solid curve denotes the calculated spectrum using parameters of $J_a = -0.044$ meV, $J_b = 0.35$ meV, $J_c = 10.4$ meV, and $E_A = 0.13$ meV. A dashed one denotes the calculated spectrum using parameters of $J_a = -0.050$ meV, $J_b = 0.50$ meV, $J_c = 9.02$ meV, and $E_A = 0.15$ meV.

In other kinds of excitation a bound state was observed by Raman scattering, for example, that of two rotons in liquid helium.[15] When the attractive interaction is not so strong, a resonance state is formed near the bottom of the continuous band spectrum. Sekine, Uchinokura, and Matsuura[16] observed a resonant state of two soft phonons in $SrTiO_3$ by Raman scattering. The two-phonon bound and resonance states were theoretically studied by Ruvalds and Zawadowski.[17] In the case of two-phonon Raman scattering, they showed that the intensity is transferred to the bound state, and we should observe a peak instead of the M_0-type Van Hove singularity in the Raman scattering.

Sugai[12] reported that the 30-cm^{-1} peak is a soft-phonon mode related to the spin-Peierls transition. He claimed that a soft-zone-boundary-phonon mode was observed at 34 cm^{-1} even at 300 K because of strong fluctuation of dimerization, but we did not observe a peak around 34 cm^{-1} above T_{SP}. Lorenzo *et al.*[22] did not observe this soft-phonon mode by means of inelastic neutron scattering.

Next, the 270-cm^{-1} peak in the calculated curve (solid one) is slightly higher in frequency than the observed peak. The sharp peak comes from the density of states around $(0, 1, 0.75)$, and the divergence at this point in the density of states reflects one dimensionality in the magnetic exciton. When we used exchange integrals in all directions as parameters in order to fit the data of magnetic excitons[5] we consequently obtained that $J_a = -0.050$ meV, $J_b = 0.50$ meV, $J_c = 9.02$ meV, and $E_A = 0.15$ meV. The agreement between the calculated curve (dotted one) and the observed Raman spectrum becomes better, and in particular the agreement of the peak position at about 228 cm^{-1} was improved. As mentioned above, the magnetic excitons intrinsically interact with each other. Therefore the situation is very similar to that in two-magnon Raman scattering in antiferromagnets. When the interaction between antiferromagnetic magnons is taken into account, a peak due to the density of states of antiferromagnetic magnons shifts to lower frequency, and the sharp cut-off spectrum becomes dull.[14] In $CuGeO_3$, the interaction between magnetic excitons is expected to lead to the same result as in the case of antiferromagnets, and the disagreement between the calculated and the observed spectra around 228 cm^{-1} will be reduced. On the other hand, the 105-cm^{-1} peak appears in both the calculated curves, and the agreement is better in the dashed one. This peak consists of an M_1-type singularity at the $(0, 0, 0.5)$ point and an M_2-type singularity at the $(0.5, 0, 0.5)$ point.

Next let us discuss the origin of the 370- and 818-cm^{-1} peaks. Very recently, the superlattice reflections due to lattice dimerization caused by the spin-Peierls transition were observed at $(h/2, k, l/2)$, when h, k, and l were odd integers, by means of electron-diffraction measurement,[6] and afterwards the superlattice reflections of $(h/2, k, l/2)$, when k was an even integer, were also found by neutron diffraction.[7] The neutron-diffraction experiment[7] gave

information about the displacement of atoms below T_{SP}. Hirota *et al.* concluded that the symmetry of $CuGeO_3$ in the spin-Peierls state is D_{2h}^{18} ($Bbcm$, which is equivalent to $Cmca$ in the standard orientation). Consequently the long-wavelength optical phonons can be classified as

$$\underline{8A_g + 7B_{1g} + 6B_{2g} + 9B_{3g}} \\ +5A_u + 9B_{1u} + 8B_{2u} + 5B_{3u} ,$$

where the underlined modes are Raman active. In the spin-Peierls phase, additional four A_g, three B_{1g}, three B_{2g}, and eight B_{3g} modes become Raman active. They are folded from the zone boundary to the Γ point because of the formation of the superlattice.

In our Raman-scattering measurement at 6 K only five new peaks were observed, and three of them came from the magnetic excitons as discussed before. Since the two remaining peaks are symmetric and sharp, we consider that they are the first-order Raman spectra. We think that the 370- and 818-cm^{-1} peaks were folded phonon modes due to the lattice dimerization. Since they were observed strongly in the $b(c,c)a$ geometry, we assign them as A_g modes in the spin-Peierls state. Other peaks could not be found, probably because of their very weak Raman intensities.

Since the differences between these peaks and A_g modes at 184, 339, and 857 cm^{-1} are nearly equal to the magnetic-exciton energy at the b^* zone boundary, Nishi, Fujita, and Akimitsu[5] suggested that these peaks came from second-order Raman scattering of a phonon and a magnetic exciton. In the scattering process of the 818-cm^{-1} peak, an A_g phonon would be created and a magnetic exciton would be simultaneously annihilated according to their assignment. The Raman cross section should be generally larger when a magnetic exciton is created than when a magnetic exciton is annihilated. We did not observe the former process. We, therefore, think that their assignment is not correct.

Finally, we measured the temperature dependence of Raman spectra of the 110-cm^{-1} peak in detail near T_{SP}, as shown in Fig. 7. The observed Raman peak was also fitted by Eq. (1) with $\alpha = 1$. The parameter ω_0 in Fig. 7 changed near T_{SP}. This result shows that the frequency change of the 110-cm^{-1} peak is strongly correlated with the spin-Peierls transition. According to the recent neutron scattering by Lorenzo *et al.*,[22] a spontaneous strain along the b axis appears below T_{SP}. It may be caused by the change of the bond length between atoms in the unit cell below T_{SP}. This fact probably explains the frequency change of the 110-cm^{-1} peak in the spin-Peierls state.

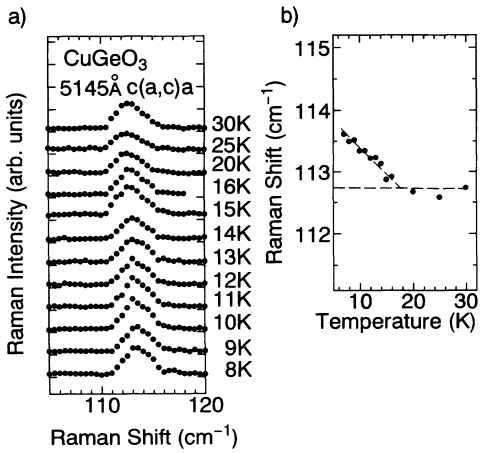

FIG. 7. (a) Temperature dependence of Raman spectrum around 110 cm^{-1} below and above T_{SP}. (b) Temperature dependence of $\omega_0(T)$ of the 110-cm^{-1} peak. Dashed lines are guides to the eye.

IV. CONCLUSION

We studied the spin-Peierls phase transition in the $CuGeO_3$ by means of Raman scattering below and above $T_{SP} = 14$ K. The number and the polarization characteristics of the observed Raman peaks indicate that the crystal symmetry of $CuGeO_3$ is D_{2h}^5 above T_{SP}. Five additional peaks were observed in the spin-Peierls state. The frequency of the peak at 30 cm^{-1} decreases with increasing temperature, and the temperature dependence agrees approximately with $2\Delta(T)$ which was obtained by neutron scattering. We assigned it as a 2Δ-gap excitation. The occurrence of a peak was explained by the bound-state formation of two magnetic excitons at the spin-Peierls gap. The Raman spectrum below 300 cm^{-1} was compared with the density of states of the magnetic exciton. The 105- and 228-cm^{-1} peaks originate from two-magnetic-exciton Raman scattering. The symmetry of the crystal at room temperature, D_{2h}^5, changes to D_{2h}^{18} at T_{SP}, and the folded A_g phonon modes were observed at 370 and 818 cm^{-1} .

ACKNOWLEDGMENTS

This study was supported in part by the Research Fellowships of Japan Society for the Promotion of Science for Young Scientists.

[1]M. Hase, I. Terasaki, and K. Uchinokura, Phys. Rev. Lett. **70**, 3651 (1993).
[2]H. Kuroe, K. Kobayashi, T. Sekine, M. Hase, Y. Sasago, I. Terasaki, and K. Uchinokura, J. Phys. Soc. Jpn. **63**, 365 (1994).
[3]M. Hase, I. Terasaki, K. Uchinokura, M. Tokunaga, N. Miura, and H. Obara, Phys. Rev. B **48**, 9616 (1993).
[4]J. C. Bonner and M. E. Fisher, Phys. Rev. **135**, A640 (1964).
[5]M. Nishi, O. Fujita, and J. Akimitsu, Phys. Rev. B **50**, 6508 (1994).
[6]O. Kamimura, M. Terauchi, M. Tanaka, O. Fujita, and J. Akimitsu, J. Phys. Soc. Jpn. **63**, 2467 (1994).
[7]K. Hirota, D. E. Cox, J. E. Lorenzo, G. Shirane, J. M. Tranquada, M. Hase, K. Uchinokura, H. Kojima, Y. Shibuya, and I. Tanaka, Phys. Rev. Lett. **73**, 736 (1994).
[8]J. P. Pouget, L. P. Regnault, M. Ain, B. Hennion, J. P. Renard, P. Veillet, G. Dhalenne, and A. Revcolevschi, Phys. Rev. Lett. **72**, 4037 (1994).
[9]H. Völlenkle, A. Wittmann, and H. Howotny, Monatsh.

Chem. **98**, 1352 (1967).
[10]D. M. Adams and P. A. Fletcher, Spectrachimica Acta **44**, 233 (1988).
[11]H. Kuroe, N. Kosugi, T. Sekine, M. Hase I. Terasaki, M. Sasago, and K. Uchinokura (unpublished).
[12]S. Sugai, J. Phys. Soc. Jpn. **62**, 3829 (1993).
[13]M. Udagawa, H. Aoki, N. Ogita, O. Fujita, A. Sohma, A. Ogihara, and J. Akimitsu (unpublished).
[14]W. Hayes and R. Loudon, *Scattering of Light by Crystals* (Wiley, New York, 1978), p. 239.
[15]T. J. Greytak and J. Yan, Phys. Rev. Lett. **22**, 987 (1969).
[16]T. Sekine, K. Uchinokura, and E. Matsuura, Solid State Commun. **18**, 569 (1976).
[17]J. Ruvalds and A. Zawadowski, Phys. Rev. B **2**, 1172 (1970). This theory was originally applied to the two-phonon Raman spectrum of diamond (Ref. 18) and they claimed that the peak observed near twice the energy of Γ point optical phonon is due to the bound state caused by anharmonic interaction (Ref. 19). Uchinokura, Sekine, and Matsuura (Ref. 20) disputed this possibility and claimed that the peak comes merely from the density of states anomaly; i.e., the maximum energy in optical phonon is located near the Γ point but not at the Γ point (Ref. 20). After that a number of papers appeared which supported their view (Ref. 21). The present authors think that the theory itself is correct in general but its application to two-phonon Raman spectrum in diamond was incorrect.
[18]Refs. 1–4 of Windl *et al.* in Ref. 21.
[19]M. H. Cohen and J. Ruvalds, Phys. Rev. Lett. **23**, 1378 (1969).
[20]K. Uchinokura, T. Sekine, and E. Matsuura, J. Phys. Chem. Solids **35**, 171 (1974).
[21]R. Tubino and J. L. Birman, Phys. Rev. Lett. **35**, 670 (1975); S. Go, H. Biltz, and M. Cardona, Phys. Rev. Lett. **34**, 580 (1975); R. Tubino and J. L. Birman, Phys. Rev. B **15**, 5843 (1977); M. Cardona, in *Light Scattering in Solids II*, edited by M. Cardona and G. Güntherodt, Vol. 50 of Topics in Applied Physics (Springer, Berlin, 1982), p. 62; P. Galtier, V. Lemos, M. Zigone, and G. Martinez, Phys. Rev. B **28**, 7334 (1983); C. Z. Wang, C. T. Chan, and K. M. Ho, Solid State Commun. **76**, 483 (1990); W. Windl, P. Pavone, K. Karch, O. Schütt, D. Strauch, P. Giannozzi, and S. Baroni, Phys. Rev. B **48**, 3164 (1993).
[22]J. E. Lorenzo, K. Hirota, G. Shirane, J. M. Tranquada, M. Hase, K. Uchinokura, H. Kojima, I. Tanaka, and Y. Shibuya, Phys. Rev. B **50**, 1278 (1994).